J Nanostruct 14(4): 1225-1238, Autumn 2024

RESEARCH PAPER

Azur C Dye Removal using GO/P(CMC-Co-Am) Nanocomposite: Adsorption and Kinetic Studies

Zaid Hamzah Abdulhusain [1], Layth S. Jasim [2], and Maryam Batool [3]*

[1] Department of Pharmaceutical Chemistry, College of Pharmacy, University of Al-Qadisiyah, Al Diwaniyah, Iraq

[2] Department of Chemistry, College of Education, University of Al-Qadisiyah, Diwaniyah, Iraq

[3] Department of Chemistry, University of Sahiwal, Sahiwal, Pakistan

ARTICLE INFO

Article History:
Received 07 July 2024
Accepted 26 September 2024
Published 01 October 2024

Keywords:
Adsorption
Azure C
GO/P(CMC-Co-Am)
nanocomposite
Kinetics

ABSTRACT

Current research deals with removing Azure C dye from aqueous solutions via adsorption on graphene oxide-carboxymethyl cellulose-co-acrylamide (GO/P(CMC-Co-Am)) nanocomposite. The nanocomposite studied here was synthesized via free radical copolymerization and further characterized by Fourier Transform infrared (FTIR), X-ray diffraction (XRD) and Field Emission electron microscopy (FESEM). For exploring the adsorption efficiency of prepared nanocomposite, batch adsorption experiments were conducted that explains the effect of pH, contact time, adsorbent dose, and salt concentration on Azure C dye adsorption. Kinetic study revealed the fitness of pseudo-second kinetic model suggesting a chemical adsorption mechanism. An optimal adsorption time of 120 minutes was observed, yielding an adsorption capacity of 9.14 mg/g. The point of zero charge of nanocomposite was observed to be pH 5. Increasing the adsorbent dose initially enhanced adsorption but eventually led to a decline due to aggregation and competition for adsorption sites. The presence of salts, particularly $CaCl_2$, positively influenced adsorption via salting-out effect.

How to cite this article
Abdulhusain Z., Jasim L., Batool M. Azur C Dye Removal using GO/P(CMC-Co-Am) Nanocomposite: Adsorption and Kinetic Studies. J Nanostruct, 2024; 14(4):1225-1238. DOI: 10.22052/JNS.2024.04.022

INTRODUCTION

The accessibility of clean and safe water is one of the most critical concerns in modern society. The key factor responsible for polluting water is industrial effluent particularly the effluent coming from textile industry [1]. Wastewater coming out from the textile sectors constitutes variety of pollutants including metals, ions, dyeing agents and other inorganic substances [2]. Among these, dyes are the common pollutants that are visible even at very less concentration and are resistant to degradation [3-8]. These dye when present in water, responsible for deteriorating water quality and all life forms on earth both directly and indirectly [9]. Azure C (Basic Violet 3) is a cationic dye that find extensive uses in dying process with its chemical formula as $C_{13}H_{12}ClN_3S$ (λ_{max} = 611.5 nm) [10, 11]. Inspite of its beneficial uses, this dye is responsible for affecting both environment and humans when it gets discharged into waterbodies without any treatment [12]. Keeping in view the toxicity caused by dye, this study is devoted to the adsorption of Azure C dye from water by adsorption technique. The simple and effective nature of adsorption process and easy availability of adsorbing agents [13-16] make this technique as superior to other available water treatment techniques [3-8, 13-15, 17-24]. The adsorbent used

* *Corresponding Author Email: layth.alhayder@gmail.com*

in the study was graphene oxide-carboxymethyl cellulose-co-acrylamide (GO/P(CMC-Co-Am)) nanocomposite that was synthesized by free radical copolymerization. The key objectives of the study include *(i)* synthesis of graphene oxide-carboxymethyl cellulose-co-acrylamide (GO/P(CMC-Co-Am)) nanocomposite by free radical copolymerization, *(ii)* characterization of prepared nanocomposite by FTIR, XRD and FESEM techniques, *(iii)* batch adsorption study for investigating the effect of pH (on both adsorption of dye and swelling ratio of adsorbent), time and salt on Azure C dye adsorption, *(iv)* investigating the kinetic modeling of dye adsorption process, providing valuable insights into the rate of adsorption.

MATERIALS AND METHODS

Materials and chemicals used

The materials and chemicals that were utilized for adsorption of Azur C dye include sodium chloride, potassium chloride, graphite (5µm), hydrochloric acid, calcium chloride, potassium persulfate, bis-acrylamide, acrylamide, carboxymethyl cellulose sodium salt, nitrogen gas, sodium nitrate, potassium permanganate, hydrogen peroxide and barium chloride.

Synthesis of hydrogel P(CMC-Co-Am)

To synthesize P(CMC-Co-Am) hydrogel, free radical copolymerization method was used. For this, 0.05 g sodium carboxymethyl cellulose (CMC) was dissolved in 50 mL of water that was followed by addition of 12g acrylamide to solution (in three-necked round-bottom flask) equipped with a condenser, a separatory funnel along with nitrogen gas inlet. This was followed by stirring of mixture and addition of 0.18g N, N'-methylenebisacrylamide (MBA), two drops of TAMAD and 0.12 grams of potassium persulfate (KPS) that serve as the initiator. The reaction mixture was then stirred continuously under a nitrogen atmosphere at 60°C for the time period of two hours. The resulting hydrogel was washed

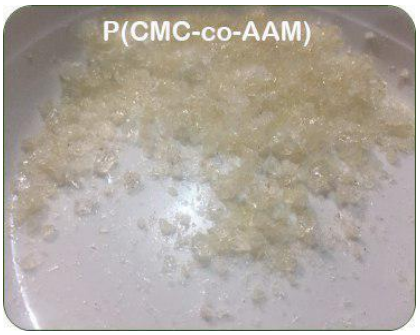

Fig. 1. Prepared hydrogel P(CMC-Co-Am).

Fig. 2. Prepared GO/P(CMC-Co-Am) nanocomposite.

repeatedly with water to remove impurities (for 6 hours with regular replacement of water after every 30 min) followed by drying in an oven at 60 °C (Fig. 1).

Synthesis of GO/P(CMC-Co-Am) nanocomposite

After the synthesis of hydrogel was done, the next step is to synthesize its nanocomposite via free radical copolymerization. For the synthesis of nanocomposite, CMC was firstly dissolved in water, followed by addition of acrylamide in a three-necked round-bottom flask equipped with a condenser, a separatory funnel, and a nitrogen gas inlet. The mixture was then stirred continuously and pre-dissolved graphene oxide (GO) was added to above mixture that was then followed by addition of KPS to mixture with continuous stirring under nitrogen at 60°C for the time period of 2 hours. The resulting nanocomposite was then cut into smaller pieces, washed and oven-dried at 60°C till a constant weight was obtained (Fig. 2).

Characterization of adsorbent

The prepared nanocomposite then undergoing characterization analysis by using three different techniques i.e., *(i)* Fourier Transform Infrared (FTIR, Shimadzu 8400s spectrophotometer within range of 500 to 4000 cm^{-1} for functional group determination [3, 22, 25]), *(ii)* Field Emission Scanning Electron Microscopy (FESEM, TESCAN MIRA3 at 25 kV voltage for morphological study [26, 27]) and *(iii)* X-ray diffraction (XRD, Shimadzu XRD-6000 at 2θ of 10° to 80° for crystallographic analysis of adsorbent [28, 29]).

Adsorption experiments

For studying the effect of equilibrium time, the time for adsorption varied from 1 to 240 min using 0.1g of adsorbent dose with neutral pH for 100 mg/l solution. The effect of pH on adsorption of Azur C dye studied via changing solution pH (from 1.2 to 10) for 50 mg/l dye solution while using 0.1g of adsorbent dose. The optimization of adsorbent dose was carried out by using solution concentration of 50 ppm at variable adsorbent doses from 0.01g to 0.08g while the study of salt (NaCl, KCl and $CaCl_2$) was carried out with 50 mg/l dye solution using 0.1g of adsorbent dose. All experiments were conducted at 20°C temperature with shaking speed of 130 rpm for 120 min (unless otherwise specified). After equilibrium time, adsorption capacity was calculated by using Eq. 1:

$$q_e = \frac{C_0 - C_e}{M} \times V \quad (1)$$

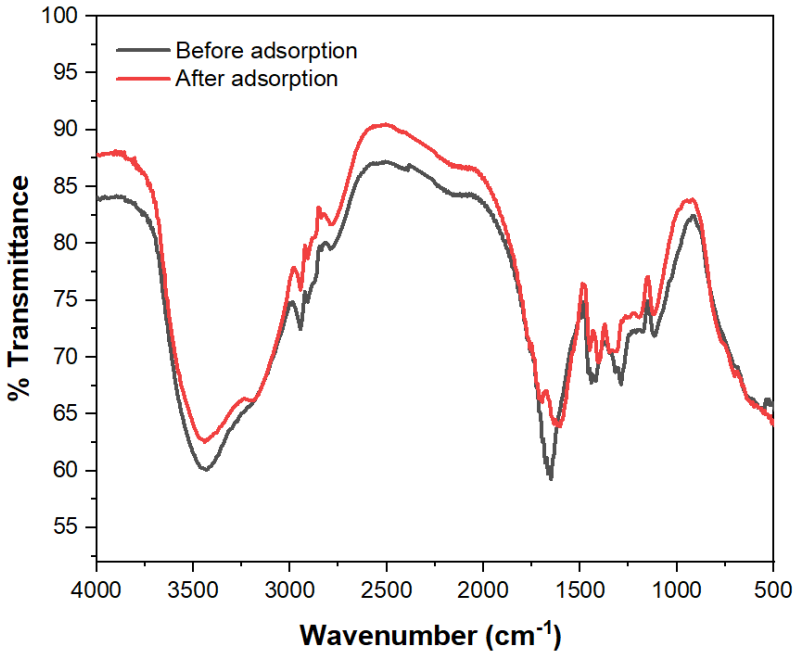

Fig. 3. FTIR of GO/P(CMC-Co-Am) nanocomposite both before and after Azure C dye adsorption.

here and denotes initial and equilibrium dye concentrations (mg/l), and denotes volume (mL) of solution as well as dose of adsorbent (g), correspondingly. The point of zero charge (pH_{PZC}) of nanocomposite determination was carried out via pH titration method. A NaCl solution was prepared and adjusted to different pH values, then mixed with the nanocomposite. The final pH of solutions measured. The graph of pH change against initial pH was plotted. The pH_{PZC} was identified as pH of intersection on this plot [30]. For studying the effect of pH on swelling percentage of prepared nanocomposite, weighed amount of adsorbent (0.1g) was immersed in solutions with variable pH ranging from 3-10. After the immersion period, the nanocomposite was filtered to remove excess water and reweighed. Swelling ratios were subsequently calculated according to the specified Eq. 2:

$$\text{Swelling ratio } (\%) = \frac{W_S - W_d}{W_d} \times 100 \quad (2)$$

where, and refers to swollen as well as dry weight (g) of nanocomposite correspondingly. The data from contact time study was applied to kinetic models. The pseudo-first-order model assumes that the rate of adsorption and number of active sites of adsorbent have direct relation with each other. Pseudo-second model presumes that rate of adsorption is proportional to square of number of adsorbent's active sites. The mathematical expressions for pseudo-first and pseudo second kinetic models are expressed in Eqs. 3 and 4 respectively:

$$\log(Q_e - Q_t) = \log Q_e - \frac{k_1}{2.303} t \quad (3)$$

$$\frac{t}{Q_t} = \frac{1}{k_2 Q_e^2} + \frac{t}{Q_e} \quad (4)$$

where (mg/g) and (mg/g) refers to amount of dye getting adsorbed at time (min) and at equilibrium, correspondingly while (1/min) and (g/mgmin) refers to rate constant for pseudo-first and pseudo-second model correspondingly [31].

RESULTS AND DISCUSSION

Characterization results

The FTIR spectrum of the GO/P(CMC-Co-Am) nanocomposite before adsorption (Fig. 3, black line) exhibited characteristic peaks at approximately 3400 cm^{-1} (hydroxyl stretching),

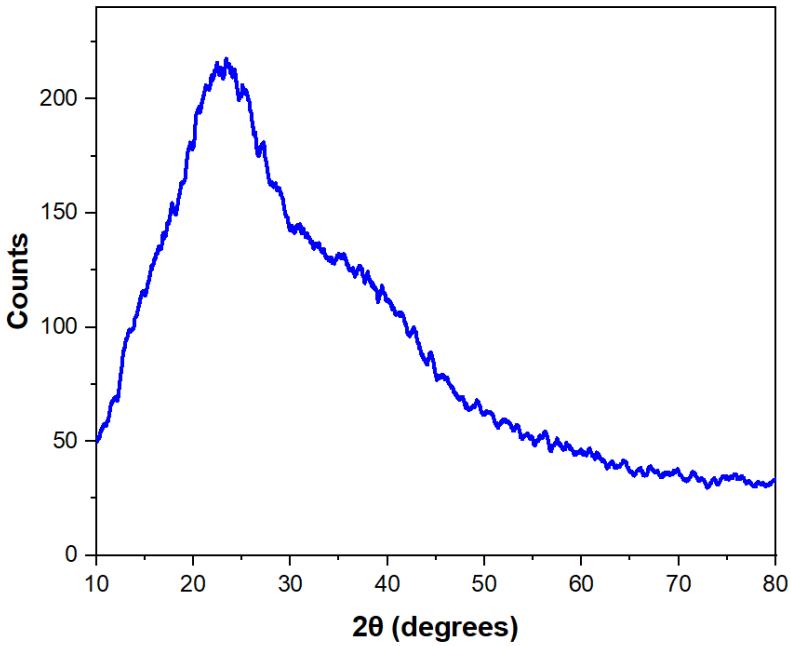

Fig. 4. XRD results of prepared GO/P(CMC-Co-Am) nanocomposite.

1700 cm^{-1} (carbonyl stretching), and 1600 cm^{-1} (aromatic C=C stretching). After the adsorption of Azure C dye (Fig. 3, red line), several changes were observed [32-34]. The intensity of 3400 cm^{-1} peak decreased, suggesting the involvement of hydroxyl groups in interactions with dye. The 1700 cm^{-1} peak shifted slightly, indicating potential interactions with carbonyl groups. The 1600 cm^{-1} peak showed minor changes, signifying π-π stacking interactions between aromatic rings of dye and GO. In fingerprint region (1000-1500 cm^{-1}), several peaks underwent changes in intensity or wavenumber, indicating the participation of other functional groups, such as C-O and C-N, in adsorption process [10, 29, 35-40].

The XRD pattern of GO/P(CMC-Co-Am) nanocomposite (Fig. 4) showed a broad peak centered around 2θ of 20-30°, indicating an amorphous or semi-crystalline structure. The absence of sharp peaks at higher angles confirmed the limited crystallinity of the nanocomposite, with the polymer contributing to its overall amorphous nature. This pattern indicated the successful incorporation of GO into polymer matrix [41-43].

The FESEM images of GO/P(CMC-Co-Am) nanocomposite before adsorption (Fig. 5a) showed a rough and porous surface morphology, which is favorable for adsorption. The nanocomposite exhibited clusters of irregularly shaped particles in nanometer range (59.59 nm) and a high surface area, which is advantageous for facilitating dye adsorption. After adsorption, however, the FESEM images revealed significant changes in surface morphology (Fig. 5b), with the previously observed rough and porous surface appearing partially covered or filled. The post-adsorption images exhibited a more compact structure with reduced pore visibility, indicating that dye molecules had occupied the available surface area, leading to decreased porosity (27.87 nm). Overall, the

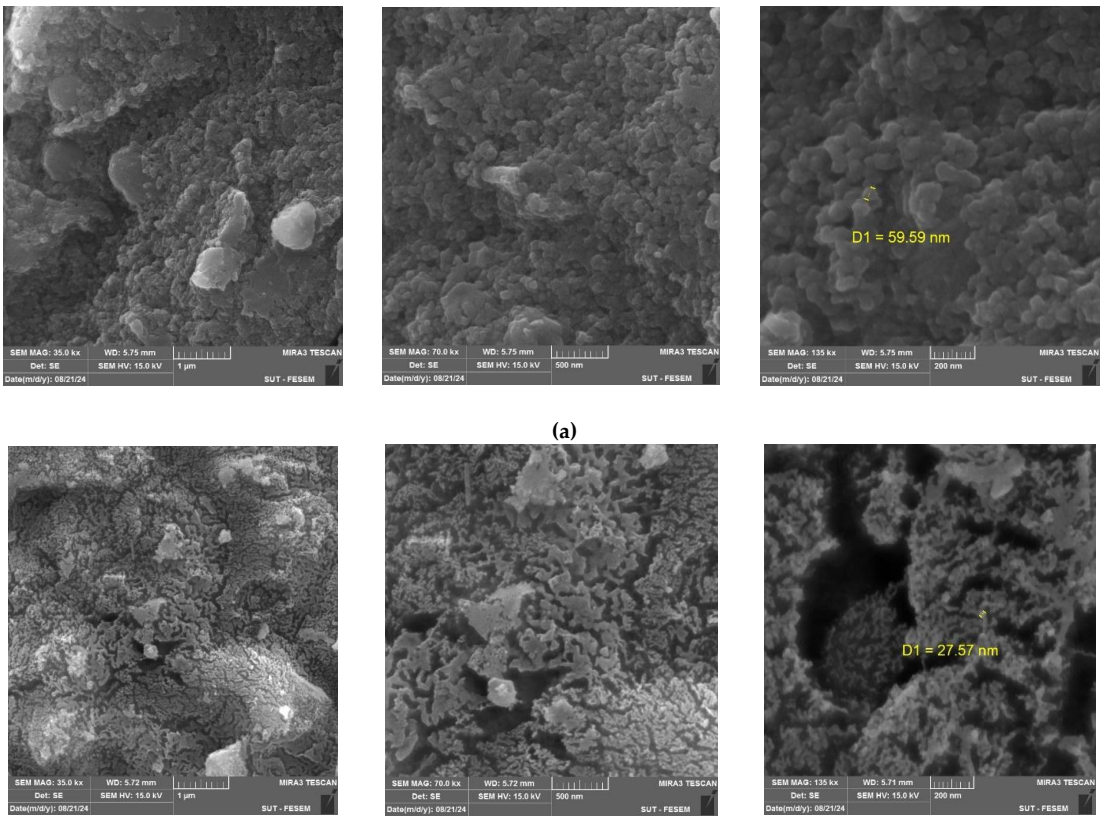

Fig. 5. FESEM of nanocomposite both (a) before and (b) after Azure C dye adsorption

results of study confirmed successful adsorption, characterized by clear surface modifications and filling of the porous structure following dye interaction [5].

Kinetic results

The graph (Fig. 6 and Table 1) revealed that the adsorption of Azure C dye onto GO/P(CMC-Co-Am) nanocomposite initially increases rapidly with time, then slows down and eventually reaches equilibrium. This is because the available active sites on nanocomposite surface are rapidly occupied by the dye molecules at the beginning. As the adsorption process continues, the number of available adsorption sites decreases, leading to a slower rate of adsorption [44].

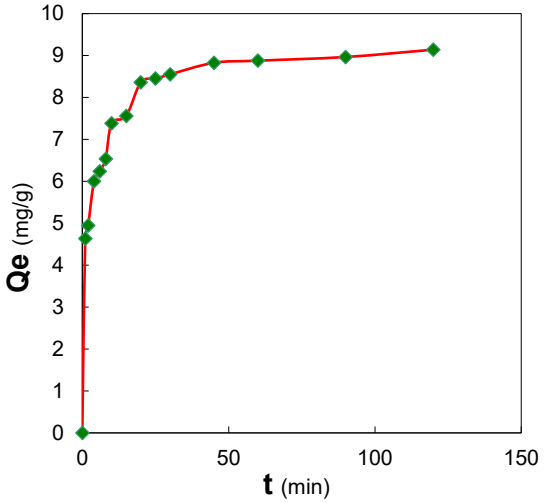

Fig. 6. Adsorption of Azure C dye onto prepared GO/P(CMC-Co-Am) nanocomposite at variable time.

Fig. 6. Adsorption of Azure C dye onto prepared GO/P(CMC-Co-Am) nanocomposite at variable time.

Time (min)	q_e (mg/ g)
0	0
1	4.634941
2	4.949902
4	6.003051
6	6.239272
8	6.534547
10	7.381004
15	7.558169
20	8.363287
25	8.449902
30	8.55128
45	8.827854
60	8.878051
90	8.96565
120	9.140846
180	9.180217
240	9.286516

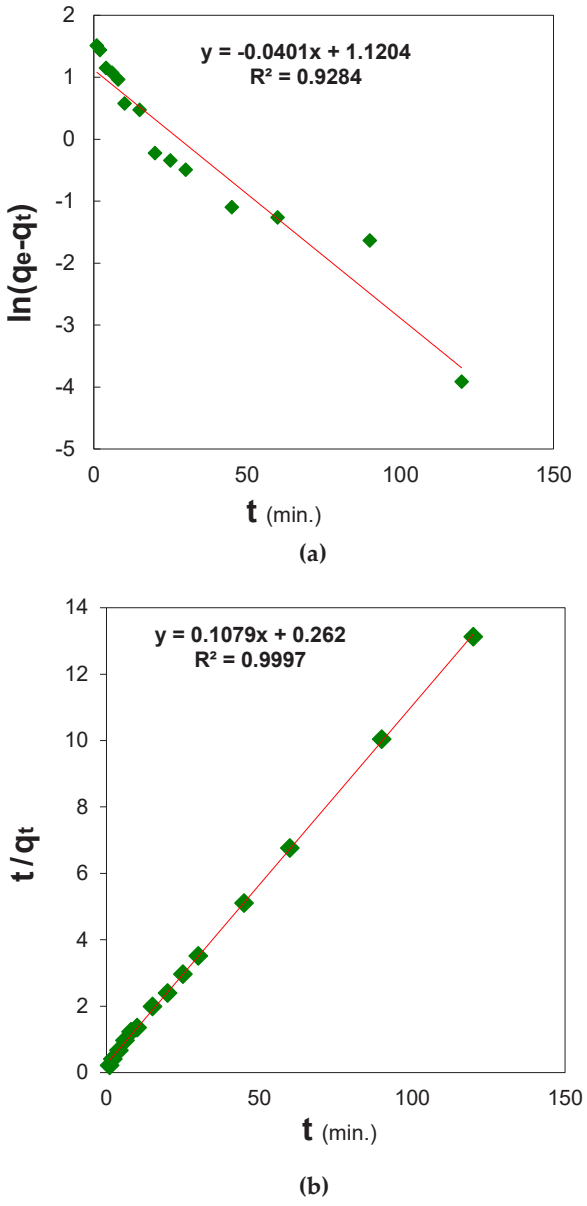

Fig. 7. Plot of (a) pseudo first and (b) pseudo second model for adsorption of Azure C dye onto prepared GO/P(CMC-Co-Am) nanocomposite.

Table 2. Parameters calculated from kinetic models i.e., pseudo first and pseudo second models. Experimental (mg/g) ws observed to be 9.14 mg/g.

Model	Pseudo-first order	Pseudo-second order
q_e (mg/g)	3.06	9.26
R^2 values	0.9284	0.9997
Constant	0.0401	0.0444
	$K_1(1/\min)$	K_2 (g/mg · min)

The nanocomposite achieved an equilibrium adsorption capacity of approximately 9.14 mg/g within 120 minutes. Although a slight increase to 9.28 mg/g was observed after an additional 120 minutes, this change was deemed insignificant. Therefore, 120 minutes was determined to be the optimal adsorption time.

The straight line pseudo first order model (Fig. 7a and Table 2) with R^2 value of 0.9284 indicates that adsorption of Azure C dye onto GO/P(CMC-Co-Am) nanocomposite is favorable. However, while comparing the values of calculated q_e (mg/g) i.e., 3.06 mg/g with experimental q_e (mg/g) i.e., 9.14 mg/g, it was observed that greater variation exists between these values. These results highlight that some other models also required for understanding the adsorption process. The results of pseudo second order model (Fig. 7band Table 2) revealed higher R^2 value of 0.9997 with minor variation between calculated q_e (mg/g) i.e., 9.26 mg/g and experimental q_e (mg/g) i.e., 9.14 mg/g. These results highlight that adsorption of Azure C dye onto the GO/P(CMC-Co-Am) nanocomposite follows pseudo-second model.

Effect of pH

The adsorption of azure C dye onto GO/P(CMC-Co-Am) nanocomposite is significantly influenced by the solution's pH (Fig. 8 and Table 3). Under acidic conditions, the nanocomposite's

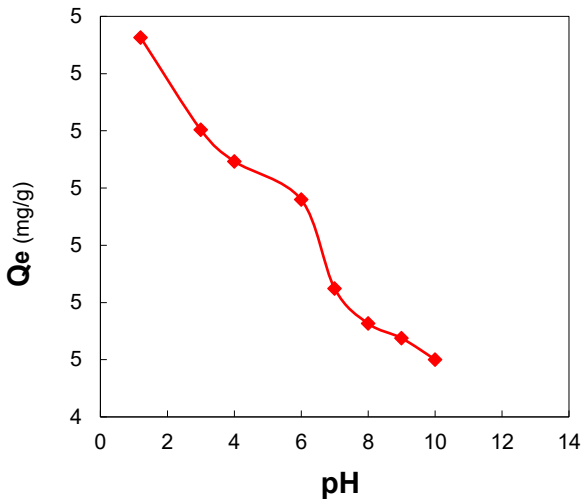

Fig. 8. Adsorption of Azure C dye onto prepared GO/P(CMC-Co-Am) nanocomposite at variable pH.

Table 3. Effect of solution pH on Azure C dye removal onto prepared GO/P(CMC-Co-Am) nanocomposite.

pH	q_e (mg/ g)
1.2	4.781594488
3	4.700885827
4	4.673326772
6	4.639862205
7	4.562106299
8	4.531594488
9	4.518799213
10	4.500098425

surface exhibits higher adsorption capacity (mg/g) compared to neutral or alkaline pH. As the pH increases, the nanocomposite's surface charge becomes less positive or even negative, reducing electrostatic attraction and hindering dye adsorption. Additionally, hydroxide ions compete with dye molecules for available adsorption sites at higher pH values. The decrease in adsorption capacity in basic pH suggests a shift in interaction mechanism, likely related to changes in the charge properties of both nanocomposite and dye. In general, adsorption of azure C dye onto GO/P(CMC-Co-Am) nanocomposite is most effective in acidic environments [44].

The point of zero charge (pH_{PZC}) is pH at which the surface charge of a material is neutral. In this study, the pH_{PZC} can be estimated by finding the pH at which the curve intersects the pH axis. Based

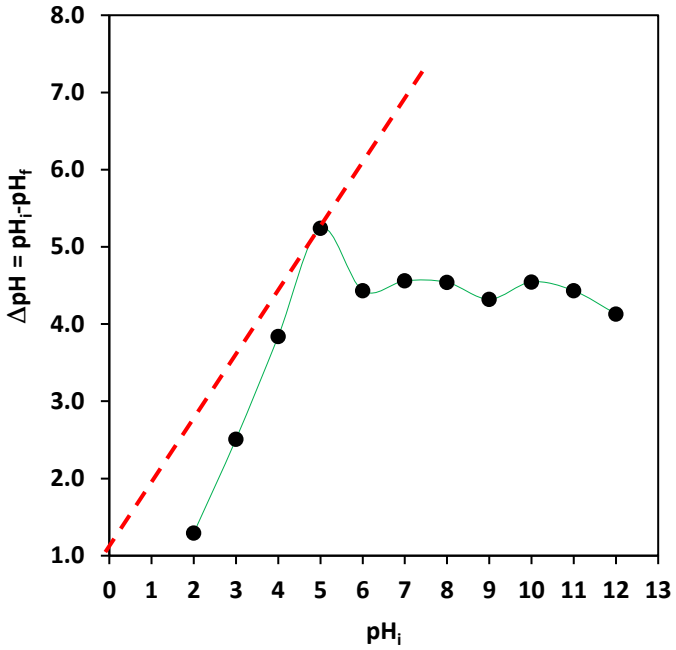

Fig. 9. pH_{PZC} determination of prepared GO/P(CMC-Co-Am) nanocomposite.

Table 4. pH_{PZC} determination of prepared GO/P(CMC-Co-Am) nanocomposite.

pH_i	pH_f
2	1.29417
3	2.50905
4	3.84039
5	5.241
6	4.433
7	4.56
8	4.54
9	4.322
10	4.546
11	4.432
12	4.131

on the results obtained, pH_{PZC} of material was around pH 5. This means that at pH value below 5, the surface of material has a net positive charge, while at pH above 5, the surface has a net negative charge. At pH_{PZC}, surface charge is neutral (Fig. 9 and Table 4).

The effect of pH was also explored on the swelling ratio of adsorbent and graph (Fig. 10 and Table 5) illustrates the influence of pH on swelling ratio of material. As pH increases from 3 to 10, the swelling ratio continuously increases. This suggests that the material's swelling behavior is sensitive to changes in pH. At lower pH values, the material exhibits a relatively low swelling ratio, indicating a more compact structure. As the pH increases, the material's structure likely undergoes changes

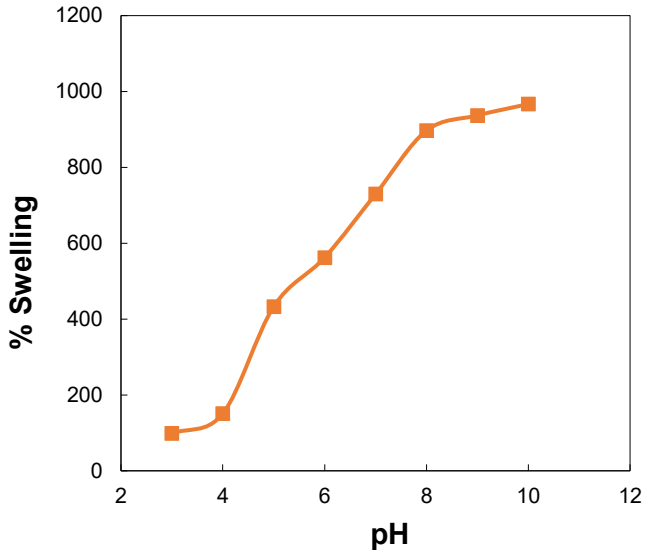

Fig. 10. Effect of pH on swelling ratio of prepared GO/P(CMC-Co-Am) nanocomposite.

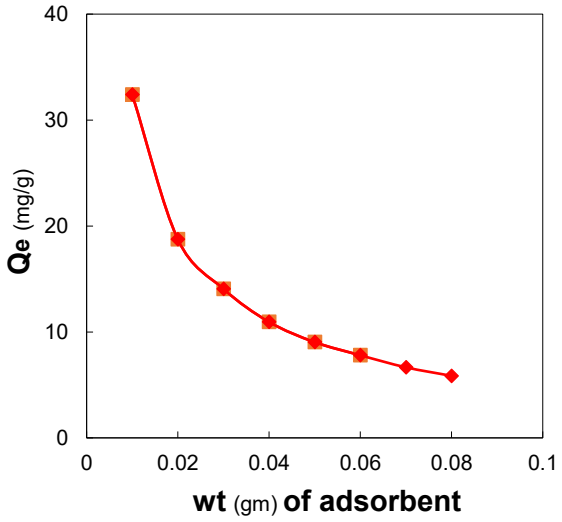

Fig. 11. Adsorption of Azure C dye onto GO/P(CMC-Co-Am) nanocomposite at variable doses of adsorbent.

that allow for greater water uptake, resulting in a significant increase in swelling ratio from 97.5% to 1648% when pH increases from 3 to 10 respectively [45].

Effect of nanocomposite dose and salt

Results of adsorbent dose (Fig. 11 and Table 6) on Azure C dye adsorption revealed that adsorption capacity (mg/g) of nanocomposite is the highest

Table 5. Effect of pH on swelling ratio of prepared GO/P(CMC-Co-Am) nanocomposite.

pH	Swelling %
3	97.5
4	253.2
5	460.0
6	890.0
7	1200.0
8	1510.0
9	1621.0
10	1648.0

Table 6. Adsorption of Azure C dye onto GO/P(CMC-Co-Am) nanocomposite at variable doses of adsorbent.

Adsorbent dose (g)	Q_e (mg/g)
0.01	32.40256
0.02	18.74065
0.03	14.06278
0.04	10.94267
0.05	9.037598
0.06	7.79872
0.07	6.659308
0.08	5.853962

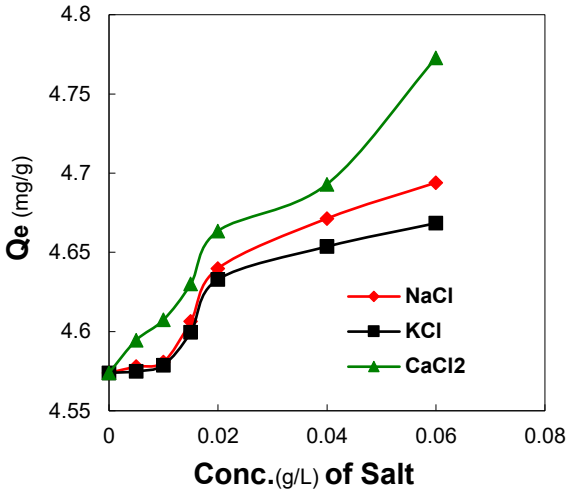

Fig. 12. Adsorption of Azure C dye onto GO/P(CMC-Co-Am) nanocomposite at variable salt concentrations.

Table 7. Adsorption of Azure C dye onto GO/P(CMC-Co-Am) nanocomposite at variable salt concentrations.

Time (min)	q_e (mg/ g)
0	0
1	4.634941
2	4.949902
4	6.003051
6	6.239272
8	6.534547
10	7.381004
15	7.558169
20	8.363287
25	8.449902
30	8.55128
45	8.827854
60	8.878051
90	8.96565
120	9.140846
180	9.180217
240	9.286516

(32.40 mg/g) at the lowest adsorbent dose (0.01g). This is because there is a greater number of available active sites on the nanocomposite surface to adsorb dye molecules. However, as the adsorbent dose continues to increase, the adsorption capacity begins to decrease (5.85 mg/g while using 0.08g of adsorbent dose). This is likely due to the aggregation of nanocomposite particles at higher concentrations, which reduces the effective surface area available for adsorption. Additionally, the competition for adsorption sites between the dye molecules may also become more intense at higher adsorbent doses, leading to a decrease in adsorption capacity [45, 46].

Results of the effect of salt concentration on adsorption of Azure C dye onto prepared GO/P(CMC-Co-Am) nanocomposite are outlined in Fig. 12 and Table 7. Study highlights the increase in adsorption capacity with increasing salt concentration for all three salts. However, the rate of increase varies among different salts. $CaCl_2$ shows the highest increment in adsorption capacity with increasing salt concentration, followed by NaCl and KCl. This trend can be attributed to the salting-out effect, where the addition of salts to a solution reduces the solubility of the adsorbed substance, thereby increasing its adsorption onto the studied adsorbent. The higher charge density of $CaCl_2$ in comparison to NaCl and KCl majorly contributes to its stronger salting-out effect thereby resulting in an increase in adsorption capacity (mg/g).

CONCLUSION

The research focuses on exploring the adsorptive capacity of a graphene oxide-carboxymethyl cellulose-co-acrylamide (GO/P(CMC-Co-Am)) nanocomposite for adsorption of Azure C dye from solution. Characterization techniques, such as FTIR, XRD, and FESEM, confirmed the successful synthesis of nanocomposite. Batch adsorption results revealed the equilibrium time to be 120 minutes and the process follows pseudo-second-order model, demonstrating a chemical adsorption mechanism. The nanocomposite can effectively adsorb dye even at low adsorbent doses. The presence of salts, particularly $CaCl_2$, enhanced adsorption capacity through the salting-out effect. Overall, the results revealed the promising potential of GO/P(CMC-Co-Am) as an efficient adsorbent for adsorptive removal of cationic dyes like Azure C dye from water.

CONFLICT OF INTEREST

The authors declare that there is no conflict of interests regarding the publication of this manuscript.

REFERENCES

1. Nawaz H, Umar M, Ullah A, Razzaq H, Zia KM, Liu X. Polyvinylidene fluoride nanocomposite super hydrophilic

membrane integrated with Polyaniline-Graphene oxide nano fillers for treatment of textile effluents. J Hazard Mater. 2021;403:123587.
2. Fu J, Zhu J, Wang Z, Wang Y, Wang S, Yan R, et al. Highly-efficient and selective adsorption of anionic dyes onto hollow polymer microcapsules having a high surface-density of amino groups: Isotherms, kinetics, thermodynamics and mechanism. Journal of Colloid and Interface Science. 2019;542:123-135.
3. Batool M, Javed T, Wasim M, Zafar S, Din MI. Exploring the usability of Cedrus deodara sawdust for decontamination of wastewater containing crystal violet dye. Desalination and Water Treatment. 2021;224:433-448.
4. Ghzal Q, Javed T, Batool M. Potential of easily prepared low-cost rice husk biochar and burnt clay composite for the removal of methylene blue dye from contaminated water. Environmental Science: Water Research & Technology. 2023;9(11):2925-2941.
5. Mannan HA, Nadeem R, Bibi S, Javed T, Javed I, Nazir A, et al. Mesoporous activated TiO_2/based biochar synthesized from fish scales as a proficient adsorbent for deracination of heavy metals from industrial efflux. J Dispersion Sci Technol. 2022;45(2):329-341.
6. Kanwal F, Javed T, Hussain F, Wasim M, Batool M. Enhanced dye photodegradation through ZnO and ZnO-based photocatalysts doped with selective transition metals: a review. Environmental Technology Reviews. 2024;13(1):754-793.
7. Saadallah K, Ad C, Djedid M, Batool M, Benalia M, Saadallah S, et al. Potential of the Algerian pine tree bark for the adsorptive removal of methylene blue dye: Kinetics, isotherm and mechanism study. J Dispersion Sci Technol. 2024:1-19.
8. Alzayd A, et al., Isotherm and Thermodynamic Analysis of Azur C Dye Adsorption on GO/P (CMC-Co-Am) Nanocomposite. Journal of Nanostructures, 2024. 14(3): p. 845-856.
9. Shi X, Wang C, Zhang J, Guo L, Lin J, Pan D, et al. Zwitterionic glycine modified Fe/Mg-layered double hydroxides for highly selective and efficient removal of oxyanions from polluted water. Journal of Materials Science & Technology. 2020;51:8-15.
10. Studies on Removal of Methylene Blue Dye from Aqueous Solution by Adsorption Using Low Cost Adsorbent. Knowledge of Research. 2016.
11. The value of iron supplementation to children with Helicobacter pylori infection in Iraq: a cross-sectional study. International Journal of Pharmaceutical Research. 2020;12(02).
12. Ibrahim HK, Albo Hay Allah MA, Al-Da'amy MA, Kareem ET, Abdulridha AA. Adsorption of Basic Dye Using Environmental friendly adsorbent. IOP Conference Series: Materials Science and Engineering. 2020;871(1):012027.
13. Arshad R, Javed T, Thumma A. Exploring the efficiency of sodium alginate beads and Cedrus deodara sawdust for adsorptive removal of crystal violet dye. J Dispersion Sci Technol. 2023;45(12):2330-2343.
14. Javed T, Thumma A, Uddin AN, Akhter R, Babar Taj M, Zafar S, et al. Batch adsorption study of Congo Red dye using unmodified Azadirachta indica leaves: isotherms and kinetics. Water Practice & Technology. 2024;19(2):546-566.
15. Rehman H, Javed T, Thumma A, Uddin AN, Singh N, Baig MM, et al. Potential of easily available low-cost raw cotton for the elimination of methylene blue dye from polluted water. Desalination and Water Treatment. 2024;318:100319.
16. Khorasanizadeh MH, Hajizadeh-Oghaz M, Khoobi A, Ganduh SH, Mahdi MA, Abdulsahib WK, et al. Synthesis and characterization of HoVO4/CuO nanocomposites for photodegradation of methyl violet. Int J Hydrogen Energy. 2022;47(46):20112-20128.
17. Shah A, Arjunan A, Thumma A, Zakharova J, Bolarinwa T, Devi S, et al. Adsorptive removal of arsenic from drinking water using KOH-modified sewage sludge-derived biochar. Cleaner Water. 2024;2:100022.
18. Shah A, Zakharova J, Batool M, Coley MP, Arjunan A, Hawkins AJ, et al. Removal of cadmium and zinc from water using sewage sludge-derived biochar. Sustainable Chemistry for the Environment. 2024;6:100118.
19. Mittal H, Al Alili A, Alhassan SM. High efficiency removal of methylene blue dye using κ-carrageenan-poly(acrylamide-co-methacrylic acid)/AQSOA-Z05 zeolite hydrogel composites. Cellulose. 2020;27(14):8269-8285.
20. Majeed HJ, Idrees TJ, Mahdi MA, Abed MJ, Batool M, Yousefi SR, et al. Synthesis and application of novel sodium carboxy methyl cellulose-g-poly acrylic acid carbon dots hydrogel nanocomposite (NaCMC-g-PAAc/ CDs) for adsorptive removal of malachite green dye. Desalination and Water Treatment. 2024;320:100822.
21. Shah A, Arjunan A, Manning G, Batool M, Zakharova J, Hawkins AJ, et al. Sequential novel use of Moringa oleifera Lam., biochar, and sand to remove turbidity, E. coli, and heavy metals from drinking water. Cleaner Water. 2024;2:100050.
22. Shah A, Arjunan A, Manning G, Zakharova J, Andraulaki I, Batool M. The effect of dose, settling time, shelf life, storage temperature and extractant on Moringa oleifera Lam. protein coagulation efficiency. Environmental Nanotechnology, Monitoring & Management. 2024;21:100919.
23. Shah A, Manning G, Zakharova J, Arjunan A, Batool M, Hawkins AJ. Particle size effect of Moringa oleifera Lam. seeds on the turbidity removal and antibacterial activity for drinking water treatment. Environmental Chemistry and Ecotoxicology. 2024;6:370-379.
24. Singh DK, Garg A. Application of sewage sludge derived hydrochar as an adsorbent for removal of methylene blue. Sustainable Chemistry for the Environment. 2024;8:100158.
25. Jiang Z, Han X, Zhao C, Wang S, Tang X. Recent Advance in Biological Responsive Nanomaterials for Biosensing and Molecular Imaging Application. Int J Mol Sci. 2022;23(3):1923.
26. Daffalla SB, Mukhtar H, Shaharun MS. Preparation and characterization of rice husk adsorbents for phenol removal from aqueous systems. PLoS One. 2020;15(12):e0243540-e0243540.
27. Shakerimoghaddam A, Majeed HJ, Hashim AJ, Abed MJ, Jasim LS, Salavati-Niasari M. Green synthesis and characterization of NiO/Hydroxyapatite nanocomposites in the presence of peppermint extract and investigation of their antibacterial activities against Pseudomonas aeruginosa and Staphylococcus aureus. Results in Chemistry. 2025;13:101947.
28. Behazin E, Ogunsona E, Rodriguez-Uribe A, Mohanty AK, Misra M, Anyia AO. Mechanical, Chemical, and Physical Properties of Wood and Perennial Grass Biochars for Possible Composite Application. BioResources. 2015;11(1).
29. Batool M, Haider MN, Javed T. Applications of Spectroscopic Techniques for Characterization of Polymer Nanocomposite: A Review. Journal of Inorganic and Organometallic Polymers

and Materials. 2022;32(12):4478-4503.
30. Malatji N, Makhado E, Ramohlola KE, Modibane KD, Maponya TC, Monama GR, et al. Synthesis and characterization of magnetic clay-based carboxymethyl cellulose-acrylic acid hydrogel nanocomposite for methylene blue dye removal from aqueous solution. Environmental Science and Pollution Research. 2020;27(35):44089-44105.
31. Saruchi, Kumar V, Ghfar AA, Pandey S. Microwave Synthesize Karaya Gum-Cu, Ni Nanoparticles Based Bionanocomposite as an Adsorbent for Malachite Green Dye: Kinetics and Thermodynamics. Frontiers in Materials. 2022;9.
32. Synthesis of Poly(methacrylic acid)/Montmorillonite Hydrogel Nanocomposite for Efficient Adsorption of Amoxicillin and Diclofenac from Aqueous Environment: Kinetic, Isotherm, Reusability and Thermodynamic Investigations. American Chemical Society (ACS).
33. Javed T, Kausar F, Zawar MD, Khalid N, Thumma A, Ismail A, et al. Investigating the adsorption potential of coconut coir as an economical adsorbent for decontamination of lanthanum ion from aqueous solution. J Dispersion Sci Technol. 2024:1-12.
34. Bayati-Komitaki N, Ganduh SH, Alzaidy AH, Salavati-Niasari M. A comprehensive review of $Co3O_4$ nanostructures in cancer: Synthesis, characterization, reactive oxygen species mechanisms, and therapeutic applications. Biomedicine and Pharmacotherapy. 2024;180:117457.
35. Moussa I, Khiari R, Moussa A, Belgacem MN, Mhenni MF. Preparation and Characterization of Carboxymethyl Cellulose with a High Degree of Substitution from Agricultural Wastes. Fibers and Polymers. 2019;20(5):933-943.
36. Leshaf A, Ziani Cherif H, Benmansour K. Adsorption of Acidol Red 2BE-NW Dye from Aqueous Solutions on Carboxymethyl Cellulose/Organo-Bentonite Composite: Characterization, Kinetic and Thermodynamic Studies. Journal of Polymers and the Environment. 2019;27(5):1054-1064.
37. Batool M, Abid MA, Javed T, Haider MN. Applications of biodegradable polymers and ceramics for bone regeneration: a mini-review. International Journal of Polymeric Materials and Polymeric Biomaterials. 2024;74(1):39-53.
38. Bukhari A, Javed T, Haider MN. Adsorptive exclusion of crystal violet dye from wastewater by using fish scales as an adsorbent. J Dispersion Sci Technol. 2022;44(11):2081-2092.
39. Imran MS, Javed T, Areej I, Haider MN. Sequestration of crystal violet dye from wastewater using low-cost coconut husk as a potential adsorbent. Water Sci Technol. 2022;85(8):2295-2317.
40. Urooj H, Javed T, Taj MB, Nouman Haider M. Adsorption of crystal violet dye from wastewater on Phyllanthus emblica fruit (PEF) powder: kinetic and thermodynamic. Int J Environ Anal Chem. 2023;104(19):7474-7499.
41. Awad MA, Jasim Al-Hayder LS. Removel of a Bsoprolol drug from Aqueous Solutions onto Graphene Oxide/ Carboymethyl cellulose sodium / Acryl acid polymer Composite by Adsorption. IOP Conference Series: Materials Science and Engineering. 2020;928(5):052033.
42. Aglawe SB. Formulation And Evaluation Of Gastroretentive Floating Dosage Form Of Nizatidine. World Journal of Pharmacy and Pharmaceutical Sciences. 2017:1345-1352.
43. Mahde BW, Sultan AM, Mahdi MA, Jasim LS. Kinetic Adsorption and Release Study of Sulfadiazine Hydrochloride Drug from Aqueous Solutions on GO/P(AA-AM-MCC) Composite. International Journal Of Drug Delivery Technology. 2022;12(04):1583-1589.
44. Abdullah AR, Jasim LS. High-efficiency removal of diclofenac sodium (DS) drug using chitosan-grafted-poly(acrylic acid-co-N-isopropylacrylamide)/kaolin clay hydrogel composite. Int J Environ Anal Chem. 2024:1-21.
45. Rafak SH, Jasim LS. Synthesis of novel bentonite/pectin-grafted-poly(crotonic acid-co-acrylic acid) hydrogel nanocomposite for adsorptive removal of safranin O dye from aqueous solution. Int J Environ Anal Chem. 2024:1-24.
46. Nipaa ST, Rahman MW, Sahaa R, Hasana MM, Deb A. Jute stick powder as a potential low-cost adsorbent to uptake methylene blue from dye enriched wastewater. Desalination and Water Treatment. 2019;153:279-287.